APPLIED GEOPHYSICS, Vol.8, No.3 (September 2011), P. 207 - 216, 5 Figures.
DOI:10.1007/s11770-011-0292-2

Multi-wave amplitude-preserved AVO modeling considering wave propagation effects

Hou Bo[1,2], Chen Xiao-Hong[1,2], Li Jing-Ye[1,2], and Zhang Xiao-Zhen[3]

Abstract: Traditional AVO forward modeling only considers the impact of reflection coefficients at the interface on seismic wave field amplitude and ignores various propagation effects. Introducing wave propagation effects including geometric spreading, transmission loss, attenuation into seismic wave propagation, multi-wave amplitude-preserved AVO forward modeling for horizontally layered media based on ray theory is proposed in this paper. We derived the multi-wave geometric spreading correction formulas for horizontally layered media in order to describe the geometric spreading effect of multi-wave propagation. Introducing the complex traveltime directly, we built the relationship between complex traveltime and quality factor without the help of complex velocity to describe the attenuation of viscoelastic media. Multi-wave transmission coefficients, obtained by solving the Zoeppritz equations directly, is used to describe the transmission loss. Numerical results show that the effects of geometric spreading, attenuation, and transmission loss on multi-wave amplitude varies with offset and multi-wave amplitude-preserved AVO forward modeling should consider the reconstructive effect of wave propagation on reflection amplitude.
Keywords: Amplitude-preserved AVO, geometric spreading, attenuation, transmission loss, complex traveltime, multi-wave

Introduction

Based on a plane wave assumption, Zoeppritz (1919) derived the reflection and transmission coefficients equations for a single formation interface with an incident P-wave called the Zoeppritz equations. To facilitate the application, some authors (Koefoed, 1955; Aki and Richards, 1980; Shuey, 1985; Gidlow et al., 1992) made linear approximations of these equations. AVO modeling based on the Zoeppritz equations and their approximations are widely used in AVO (Amplitude-versus-Offset) analysis. Ostrander (1984) calculated the AVO responses of gas sand using the Koefoed (1955) approximation and indicated it was effective to identify gas-bearing sandstones using P-wave reflection amplitude versus incident angle. Rutherford and Williams (1989) studied the AVO responses of gas sand under different geological conditions taking advantage of the Zoeppritz equations and divided these AVO responses of gas-bearing sandstone into three types, which has been widely accepted by later researchers. Castagna and Swan (1997) and Castagna et al. (1998) extended the AVO classification to four types

Manuscript received by the Editor January 31, 2011; revised manuscript received August 23, 2011.
This research work is sponsored by the National Natural Science Foundation of China (Grant No. 41074098) and the National Basic Research Program of China (973 Program) (Grant No. 2007CB209606).
1. State Key Lab of Petroleum Resource and Prospecting, Beijing 102249, China
2. CNPC Key Lab of China University of Petroleum(Beijing), Beijing 102249, China
3. Geological Scientific Research Institute of Shengli Oilfield, SINOPEC, Dongying 257015, China

and further improved the AVO response reaearch on gas sandstone, all of which laid the foundation for AVO attribute analysis. Based on the Shuey approximation, Foster et al. (2010) studied the changes of amplitude with offset when the lithology, porosity, and fluid changed. They pointed out that the change of porosity had an effect on acoustic impedance but little effect on compressional to shear wave velocity ratio.

Zoeppritz equations and their approximations are also often applied to AVO inversion. Chen et al. (2006) and Wei et al. (2008) realized converted wave and compressional wave inversion using the Aki-Richards approximation. Yang et al. (2009) and Yan and Gu (2010) researched prestack elastic parameter inversion methods using the Gidlow approximation.

AVO analysis and inversion, which stem from Zoeppritz equations or their approximations, play a significant role in lithology and fluid identification. However, all the analysis is based on the information of a single reflection interface and ignores propagation effects on seismic wave amplitudes and thus has low precision.

Elastic wave equation forward modeling for horizontally layered media (Fuchs and Muller, 1971; Kennett, 1983; Muller, 1985; Mallick and Frazer, 1987) can simulate various wave propagation effects in horizontally layered. Using elastic wave equation, wave field propagating in complex medium also can be simulated (Che et al., 2010; Lu and Wang, 2010). Elastic wave equation can simulate full-wave field recording including reflected waves, converted waves, multiples, and so on, so the amplitude of the simulated wave field has high accuracy. However, the elastic wave equation forward modeling computation is time-consuming. Inversion based on the elastic wave equation (Zhang and Yin, 2004, 2005) requires repeated iterations and then the computation cost is more expensive.

In this paper, we present a multi-wave amplitude-preserved AVO forward modeling method, taking into consideration several major wave propagation factors, including transmission loss, geometric spreading, and attenuation on wave field amplitude and giving the forward wave field amplitude higher fidelity. We call it "amplitude-preserved" AVO forward modeling in order to emphasize the difference between this method and the traditional forward modeling method based on single interfaces. The computational complexity of this method is much less than that of the forward modeling by directly solving the elastic wave equation while havin comparatively high-efficiency AVO forward modeling method which can also relatively preserve the true amplitude response of seismic waves.

Theory and method

Based on asymptotic ray theory, seismic wave fields can be expressed with ray series (Cerveny and Ravindra,1971; Cerveny et al.,1977; Cerveny and Hron,1980; Hearn and Krebest,1990):

$$\mathrm{u}(M,t)=\frac{1}{\pi}\mathrm{Re}\int_0^{\infty}\left(S(\omega)e^{i\omega[t-\tau(M)]}\sum_{n=0}^{\infty}\frac{W_n(M)}{(i\omega)^n}\right)d\omega, \quad (1)$$

Where u (M, t) is the wave field amplitude at receiver M at time t, $W_n(M)$ is the n-th order ray amplitude, ω is angular frequency, $S(\omega)$ is the wavelet Fourier spectrum.

The approximate solution of the zero-order ray series is

$$\mathrm{u}(M,t)=\frac{1}{\pi}\mathrm{Re}\int_0^{\infty}\left(S(\omega)e^{i\omega[t-\tau(M)]}W_0(M)\right)d\omega, \quad (2)$$

where

$$W_0(M)=\frac{A_0(v\rho)_{M_0}^{1/2}}{L(M)(v\rho)_M^{1/2}}\prod_{k=1}^{K-1}\left[\frac{(v\rho)_{O_{k^-}}}{(v\rho)_{O_{k^+}}}\right]^{1/2}\prod_{k=1}^{K-1}R(O_k)T(O_k), \quad (3)$$

where A_0 is the initial ray amplitude at point M_0, O_{k^-} represents the incident ray side on the k-th incident interface, O_{k^-} is the emergent ray side in the k-th interface, $(v\rho)_{O_{k^+}}$ is the impedance (product of velocity and density) at the side of the incident ray on the k-th incident interface, and $(v\rho)_{O_{k^-}}$ is the impedance at the emergent ray on the k-th incident interface. $T(O_k)$ is the transmission coefficient for the k-th interface. If the outgoing wave is a reflected wave, $T(O_k)$ is equal to 1. $R(O_k)$ is the reflection coefficient for the k-th interface. If the outgoing wave is a transmitted wave, $R(O_k)$ is equal to 1. $L(M)$ is the geometric spreading correction factor from M_0 to M, which is defined (Cerveny and Ravindra, 1971):

$$L(M)=\left[x\frac{\partial x}{\partial\theta(M_0)}\frac{\cos\theta(M)}{\sin(M_0)}\right]^{1/2}\prod_{k=1}^{K}\left[\frac{\cos\theta(O_{k^+})}{\cos\theta(O_{k^-})}\right]^{1/2}. \quad (4)$$

where x is the offset and $\theta(O_{k^+})$ and $\theta(O_{k^-})$ represent the emergent and incident angles at the k-th interface, between the vertical and the ray segment entering and leaving O_k, respectively.

Although equation (2) can describe wave propagation in complex media theoretically, the calculations become very complicated. As AVO forward modeling or inversion is usually based on the assumption of

horizontally layered media, this paper only discusses amplitude-preserved AVO forward modeling for horizontally layered media. The following focuses on discussing the several factors affecting the wave field amplitude.

Geometric spreading correction factor

The geometric spreading correction factor results from the wave front continuously spreading while the wave propagates and the wave amplitude reduces to keep the total energy constant. Using equation (4), we can obtain the geometric spreading correction factor of the PP wave (incident P-wave and reflected P-wave). The derivation of the equation is shown in Appendix A):

$$L(M)=\frac{2}{v_{p1}}\left[\sum_{i=1}^{K}\left(\frac{v_{pi}^2h_i^2}{\left(1-p^2v_{pi}^2\right)^2}\right)\cos\theta(M_0)\cos\theta(M)\right]^{1/2}. \tag{5}$$

Similarly, the geometric spreading correction factor for PS waves (incident P-wave and reflected S-wave) can be derived from equation (4) (see Appendix A):

$$L(M)=\left[\sum_{i=1}^{K}\left(\frac{v_{pi}h_i}{\left(1-p^2v_{pi}^2\right)^{1/2}}+\frac{v_{si}h_i}{\left(1-p^2v_{si}^2\right)^{1/2}}\right)\right]^{1/2}$$
$$\left[\frac{\cos\theta(M_0)\cos\theta(M)}{v_{p1}^2}\sum_{i=1}^{K}\left(\frac{v_{pi}h_i}{\left(1-p^2v_{pi}^2\right)^{3/2}}+\frac{v_{si}h_i}{\left(1-p^2v_{si}^2\right)^{3/2}}\right)\right]^{1/2}\prod_{k=1}^{K}\left[\frac{\cos\theta\left(O_{k^+}\right)}{\cos\theta\left(O_{k^-}\right)}\right]^{1/2}. \tag{6}$$

Transmission loss

Traditional AVO forward modeling based on ray tracing only calculates the reflection coefficients at the interface while ignoring the wave transmission during wave propagation. Transmission coefficients are similar to reflection coefficients and have the AVO effect, which means transmission coefficients vary with offset. In other words, transmission has different impact on the wavefield amplitude at different offsets (incident angles). Transmission changes the reflection wave AVO response characteristics. Ignoring the role of transmission, the wave field amplitude is inaccurate. In this paper, we calculate transmission coefficients at interfaces during the ray tracing and apply them to the wave field amplitude calculation, which makes the computed wave field better preserve the real wave field amplitude response. $T=\prod_{k=1}^{K-1}T(O_k)$ represents the wave field amplitude transmission loss caused when the wave propagates in horizontally layered media and passes through all the interfaces. The transmission coefficient $T(O_k)$ can be obtained from the Zoeppritz equations:

$$\begin{bmatrix}
\sin\theta_1 & \cos\varphi_1 & -\sin\theta_2 & \cos\varphi_2 \\
-\cos\theta_1 & \sin\varphi_1 & -\cos\theta_2 & -\sin\varphi_2 \\
\sin 2\theta_1 & \frac{V_{P1}}{V_{S1}}\cos 2\varphi_1 & \frac{\rho_2V^2{}_{S2}V_{P1}}{\rho_1V^2{}_{S1}V_{P2}}\sin 2\theta_2 & \frac{-\rho_2V_{S2}V_{P1}}{\rho_1V^2{}_{S1}}\cos 2\varphi_2 \\
\cos 2\varphi_1 & \frac{-V_{S1}}{V_{P1}}\sin 2\varphi_1 & \frac{-\rho_2V_{P2}}{\rho_1V_{P1}}\cos 2\varphi_2 & \frac{-\rho_2V_{S2}}{\rho_1V_{P1}}\sin 2\varphi_2
\end{bmatrix}\begin{bmatrix}R_{PP}\\R_{PS}\\T_{PP}\\T_{PS}\end{bmatrix}=\begin{bmatrix}-\sin\theta_1\\-\cos\theta_1\\\sin 2\theta_1\\-\cos 2\varphi_1\end{bmatrix}. \tag{7}$$

The impact of transmission loss maintains the reality of the AVO response characteristics and also reduces AVO analysis or inversion errors.

Forward modeling of viscoelastic media

Equation (2) is the forward modeling equation of elastic media. Introducing complex velocity, elastic media forward modeling can be extended to viscoelastic media (Hearn and Krebest, 1990: Hron and Nechtschein, 1996). Although viscoelastic media can be described by the introduction of complex velocity, the physical meaning of complex velocity is not clear. The relationship between wave field attenuation and complex velocity is complicated and not intuitive. What' s more, ray tracing in viscoelastic media needs the ratio of complex ray distance and complex velocity to derive complex travel time (Hearn and Krebest, 1990). The calculation is not only intricate but also adds a parameter with no clear physical meaning, that is, complex ray distance (Hearn and Krebest, 1990). This paper proposes a ray tracing method for viscoelastic media which has clear physical meaning and do not need to introduce complex velocity. It directly derives complex travel time from the elastic media velocity and quality factor Q which is the most commonly used parameter to describe viscoelastic media (see Appendix B)

$$\tau_c = \sum_{i=1}^{K} \tau_i \left(1 - \frac{j}{2Q}\right). \quad (8)$$

With the introduction of complex travel time, equation (2) can be written in a more generalized form (Appendix B):

$$\mathrm{u}(M,t) = \frac{1}{\pi}\mathrm{Re}\int_0^{\infty}\left(S(\omega)e^{i\omega[t-\tau_c(M)]}W_0(M)\right)d\omega. \quad (9)$$

Defined by complex travel time, the real part of complex travel time represents wave field phase changes, while the imaginary part represents wave field amplitude changes. The wave field amplitude changes in actual viscoelastic media is exactly the wave field amplitude attenuation, for which the physical meaning is clear and computation is simple.

In order to facilitate quantitative analysis of attenuation on wave field amplitude, we define formation absorption decay factor

$$decay = \exp\left(-\sum_{i=1}^{K}\frac{\omega\tau_i}{2Q_i}\right). \quad (10)$$

decay is the amplitude attenuation term caused by viscosity. The formation absorption decay factor characterizes seismic wave field amplitude changes caused by formation attenuation when different frequency components of the wavelet propagate in the viscoelastic media. Due to the attenuation shown in equation (10), the formation attenuation relates to quality factor, frequency, and travel time.

Numerical modeling

Taking the interface between the second and third layers in model 1 (model parameters in Table 1) as an example, we calculate the reciprocal of geometric spreading factor 1/L, formation absorption decay factor decay, and the formation transmission loss for different P-wave incident angles. From Figures 1a to 1d, it is clear that these three parameters all change with incident angle (or offset). That is to say, the three factors have similar AVO/AVA (Amplitude-versus-Offset/Amplitude-versus-Angle) characteristics to reflection coefficients. They have different effects on the reflected wave amplitudeswith different incident angles(or offsets). Because of geometric spreading, attenuation, and transmission effects in the real seismic wave fields during wave propagation, the AVO/AVA response characteristics of real wave fields are significantly different than the reflection coefficients calculated for the case of a single interface. The amplitude-preserved AVO/AVA forward modeling should consider all kinds of propagation effects like geometric spreading, attenuation and transmission loss. Figures 1a and 1b also show that the reciprocal of geometric spreading factor 1/L and formation absorption decay factor decay for reflected P-waves or converted-waves at the same interface both decrease with increasing incident angle, which is consistent with real wave field propagation. Comparing Figure 1b with Figure 1c, we see the formation attenuation factor changes with P-wave incidence angle are relatively larger than for converted waves. However, at the same incident angle, absolute amplitude attenuation of converted wave is larger than that of P-wave, because converted waves have a smaller quality factor. Figures 1b and 1c also show that amplitude attenuation for different frequencies is different. The higher frequencies show greater amplitude attenuation. Figure 1dshows transmission loss has a complicated effect on the wave field amplitudes. With the increment of incidence angle (offset), PP-wave transmission loss,Tpp, increases while PS-wave transmission loss,Tps,

decreases. The effect of Tps on wave field amplitude is relatively complex and there is no simple rule to follow.

Table1 The model 1parameters

	P-wave velocity (m/s)	Poisson's ratio	Density (g/cm^3)	P-wave quality factor	S-wave quality factor	Thickness (m)
1st layer	2400	0.4	2.2	100	50	2000
2nd layer	2140	0.1	2.1	50	50	10
3rd layer	2400	0.4	2.2	100	50	2000

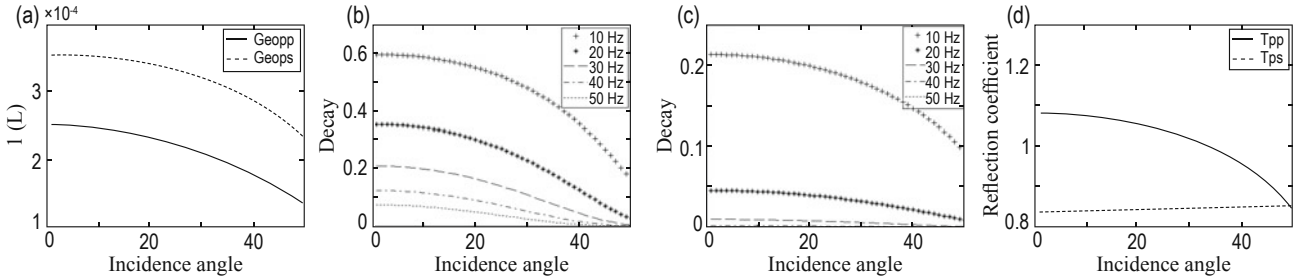

Fig. 1 The numerical results of model 1.

(a) The reciprocal of multi-wave geometric spreading factor versus incident angle (Geopp stands for PP-wave, Geops stands for PS-wave). (b) PP-wave attenuation factor for different frequencies versus incident angle. (c) PS-wave attenuation factor for different frequencies versus incident angle. (d) Multi-wave transmission loss versus incident angle (Tpp stands for PP-wave, Tps stands for PS-wave)

Figure 2a shows the multi-wave reflection coefficients AVO/AVA response of model 1 at the interface between the second and third layers. Figure 2bshows the amplitude response of reflected and converted waves including propagation effects such as geometric spreading, attenuation (at 30Hz), and transmission loss. It is the result of true amplitude preserved AVO / AVA forward modeling. In Figure 2a, the PP-wave amplitude increases with incidence angle, while in Figure 2b the PP-wave amplitude increases with incidence angle and then decreases. The PS-wave amplitude in both figures increases with incidence angle and then decreases but the peak position is different. The peak in Figure 2b has a smaller incidence angle. The higher shear wave attenuation leads to the bigger difference between P- and S-wave amplitudes. Comparing the reflection and converted wave amplitude modeling by the two AVO forward modeling methods, we know there is a significant difference in amplitude response characteristics due to propagation effects. For real AVO analysis, wave field amplitude must be corrected for geometric spreading, attenuation, and transmission loss and then the traditional AVO analysis and inversion can be applied. However, in seismic data processing, the three propagation effects are often very difficult to correct and requires accurate formation elastic parameters and quality factors, which cannot be obtained accurately. A better option is to apply multi-wave amplitude-preserved AVO forward modeling to the AVO analysis of real seismic data. As for inversion, we can modify the model by iteration based on amplitude-preserved multi-wave AVO forward modeling and iterate

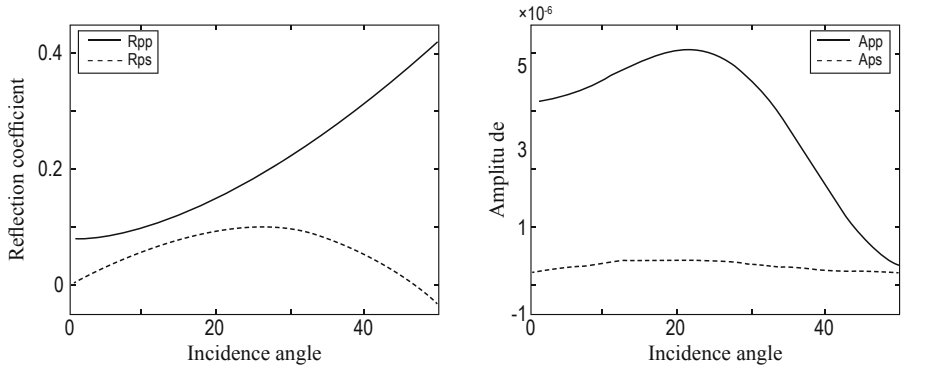

(a) Multi-wave reflection coefficients versus incident angle (Rppfor PP-wave, Rps for PS-wave).

(b) Multi-wave amplitude-preserved AVO response (App for PP-wave, Aps for PS-wave).

Fig. 2 AVO response of model 1.

the wave field computations until the forward model data fits the field seismic data well.

Figures 3a to 3e show the P-wave velocity of the horizontal layered model 2: P-wave quality factor, shear wave velocity, shear wave quality factor, and density. Figures 4a and 4c are the PP and PS seismic responses with a 30Hz source wavelet which ignores the propagation effects. Figures 4b and 4d are the PP and PS seismic responses with the same source wavelet which include the propagation effects. The seismic responses ignoring propagation effects (Figures 4a and 4c) have strong amplitude at far offset and the energy of the shallow and deep events are equivalent. On the other hand, the seismic responses considering propagation effects (Figures 4b and 4d) have noticeable amplitude attenuation at far offset and the deep events energy is obviously weaker than the shallow events. The main reason is, with increasing offset or depth, the impact of geometric spreading or attenuation on wave field amplitude increases. We see from Figure 4 the seismic response events considering propagation effects show lower dominant frequency, especially for the PS-waves. Equation (10) and Figures 1b and 1c show the attenuation effect is also related to frequency, with higher frequencies having more absorption. This causes the seismic response dominant frequency to move to lower frequencies. The shear wave quality factor is usually less than the P-wave's and, therefore, PS-waves show more attenuation and lower dominant frequency (shown in Figure 4d). In practical seismic data processing, we should consider three propagation effects on the seismic response (Figures 4b and 4d) and correct the seismic response to that ignoring the propagation effects (Figures 4a and 4c). The corrections for different frequencies, different reflection time, and different offset are all different, so accurate correction is very difficult.

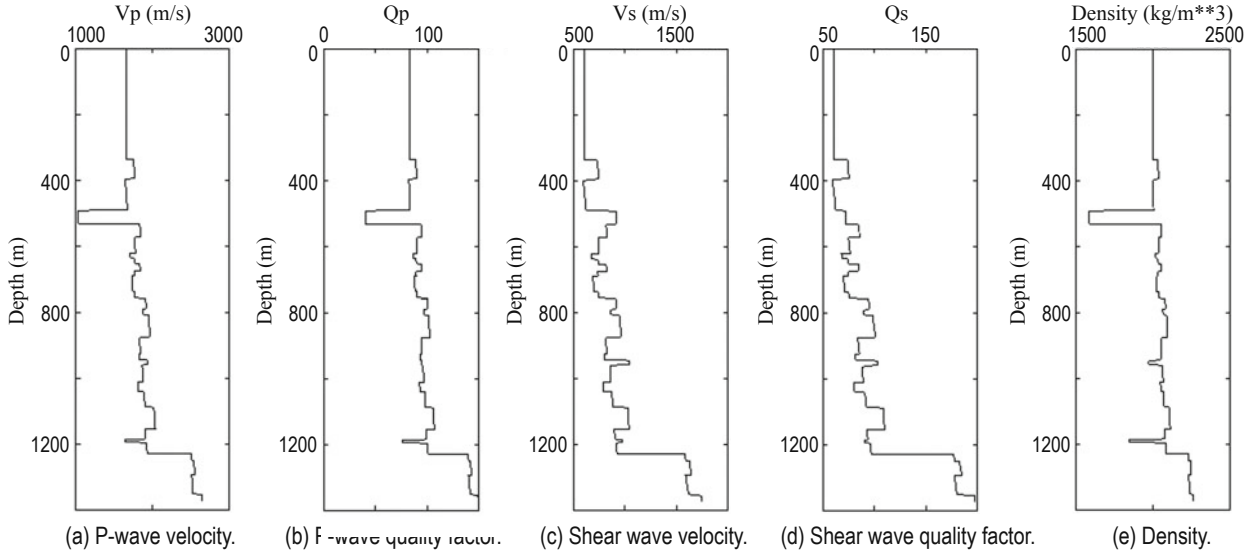

(a) P-wave velocity. (b) P-wave quality factor. (c) Shear wave velocity. (d) Shear wave quality factor. (e) Density.

Fig. 3 The parameters of model 2.

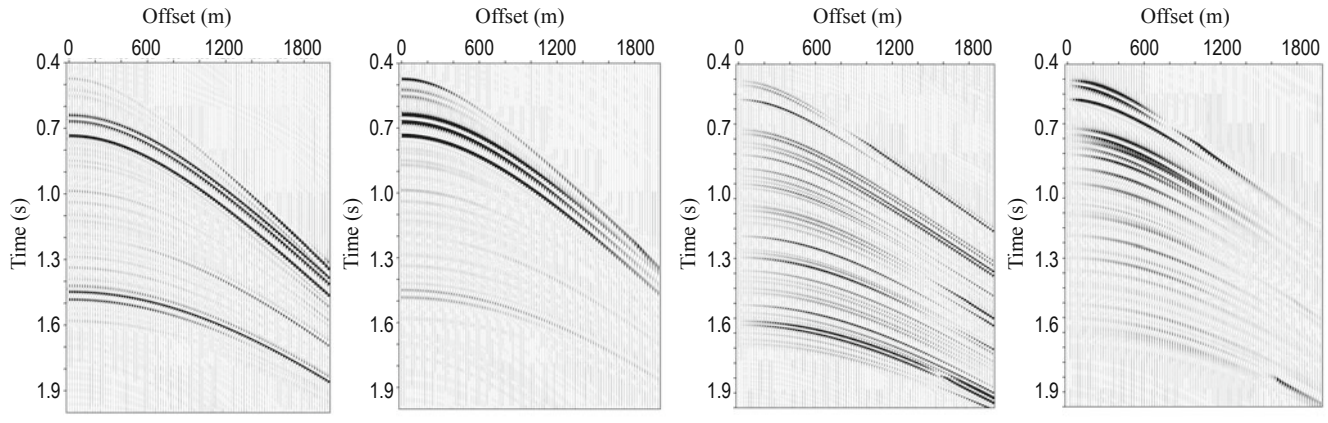

(a) PP-wave CMP gather ignoring propagation effects. (b) PP-wave CMP gather including wave propagation effects. (c) PS-wave CMP gather ignoring propagation effects. (d) PS-wave CMP gather including wave propagation effects.

Fig. 4 The seismic response of model 2.

If not corrected, seismic amplitude interpretation based on reflection coefficients is bound to have greater errors. For this reason, seismic amplitude interpretation technology based on amplitude-preserved multi-wave AVO forward modeling is more suitable for real seismic data amplitude interpretation and amplitude response characteristics studies.

Figure 5 shows a comparison of wave field amplitude simulated by elastic wave equations(Kennett, 1983; Muller, 1985; Mallick and Frazer, 1987) to that simulated by the amplitude-preserved AVO forward modeling method. The figures present reflection PP-wave amplitude(shown in Figure 5a) and converted PS-wave amplitude (shown in Figure 5b) at the interface between the second and third layers of model 3 listed in Table 2. We see from Figure 5 that the proposed amplitude-preserved AVO forward modeling method agrees with the results of elastic wave equation forward modeling very well, which proves the proposed amplitude-preserved AVO forward method to be correct and effective.

Table 2 The model 3 parameters

	P-wave velocity (m/s)	Poisson's ratio	Density (g/cm^3)	P-wave quality factor	S-wave quality factor	Thickness (m)
1st layer	2048	1202	2.14	100	50	1000
2nd layer	3048	2200	2.30	100	50	1000
3rd layer	2048	1200	2.14	100	50	1000

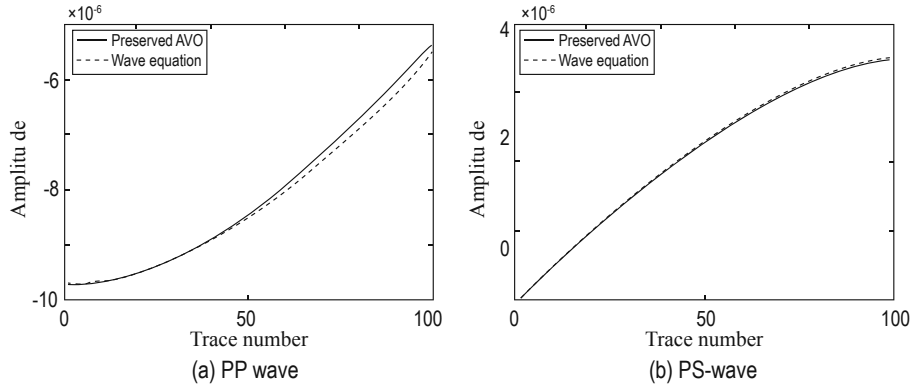

Fig. 5 Comparison of model 3 wave field amplitudes using the wave equation and amplitude-preserved AVO. (a) Solid line denotes the results of proposed amplitude-preserved AVO forward modeling, Dotted line denotes the results of wave equation forward modeling.

Conclusions

Considering the three propagation effects in real wave fields, we present a ray tracing-based multi-wave amplitude-preserving AVO modeling method. Numerical experiments show that propagation effects have great effects on multi-wave reflection amplitudes throughout wave propagation in the overlying media. The real amplitude response characteristics are significantly different than single interface reflection coefficient AVO response characteristics and, therefore, the reflection coefficient-based AVO forward modeling has large system errors for multiple wave AVO analysis and inversion. Multi-wave amplitude-preserving AVO forward modeling, compared to the reflection coefficient-based AVO forward modeling method, establishes a more precise relationship between formation parameters and seismic AVO response and has higher computational efficiency than the elastic wave equation modeling method. Multi-wave amplitude-preserving AVO forward modeling, having a high application value, can be directly applied to AVO analysis and model-based AVO inversion for field seismic data. However, it is also difficult for the proposed multi-wave amplitude-preserving AVO forward modeling to simulate multiples fast and simply, which is the subject of further research.

References

Aki, K., and Richards, P.G., 1980, Quantitative seismology: Theory and methods, Vol. 1: W.H. Freeman & Co., San Francisco, CA.

Bleistein, N., Cohen, J. K. and Stockwell, J. W., 2001,

Mathematical methods of Seismic imaging, migration and inversion: Springer-Verlag, New York.

Castagna J. P., Swan, H. W., and Foster, D. J., 1998, Framework for AVO gradient and intercept interpretation: Geophysics, **63**(3), 948 – 956.

Castagna, J. P., and Swan, H. W., 1997, Principles of AVO cross plotting: The Leading Edge, **16**, 337 – 342.

Cerveny, V., and Hron, F., 1980, The ray series method and dynamic ray tracing system for three-dimensional inhomogeneous media: Bull.Seis, Soc. Am., **70**, 47 – 77.

Cerveny, V., and Ravindra, R., 1971, Theory of seismic head waves: Univ. of Toronto Press, Canada.

Cerveny, V., Molotkov, I. A., and Psencik, I., 1977, Ray method in seismology: Charles University, Prague.

Che, C. X., Wang, X. M., and Lin, W. J., 2010, The Chebyshev spectral element method using staggered predictor and corrector for elastic wave simulations, Applied Geophysics, **7**(2), 174 – 184.

Chen, T. S., Liu, Y., and Wei, X. C., 2006, Joint amplitude versus off set inversion of P-P and P-SV seismic data: Journal of China University of Petroleum, **30**(1), 33 – 37.

Foster, D. J., Keys,R. G., and Lane, F.D., 2010, Interpretation of AVO anomalies: Geophysics, **75**(5), 75A3 – 75A13.

Fuchs, K., and Muller, G., 1971, Computation of synthetic seismograms with the reflectivity method and comparison with observations: Geophysical Journal Royal Astronomical Society, **23**, 417 – 433.

Gidlow, P. M., Smith, G. C., and Vail, P. J., 1992, Hydrocarbon detection using fluid factor traces: Joint SEG / EAGE Summer Research Workshop, Technical Program and Abstracts, 78 – 89.

Hearn, D. J., and Krebest, E. S., 1990, On computing ray-synthetic seismograms for an elastic media using complex rays: Geophysics, **55**(4), 422 – 432.

Hron, F., and Nechtschein, S., 1996, Extension of asymptotic ray theory to linear viscoelastic media: 66th Annual International Meeting, SEG, Expanded Abstracts, 1983 – 1986.

Hron, F., May, B. T., Covey, J. D., and Daley, P. F., 1986, Synthetic seismic sections for acoustic, elastic, anisotropic, and vertically inhomogeneous layered media: Geophysics, **51**(3),710 – 735.

Kennett, B. L. N., 1983, Seismic wave propagation in stratified media: New York, Cambridge University Press, London.

Koefoed, O., 1955, On the effect of Poisson's ratios of rock strata on the reflection coefficients of plane waves: Geophysical Prospecting, **3**, 381 – 387.

Lu, J. and Wang Y., 2010, Seismic wave propagation in Kelvin visco-elastic VTI media, Applied Geophysics, **7**(4), 357 – 364.

Mallick, S., and Frazer, L. N., 1987, Practical aspects of reflectivity modeling: Geophysics, **52**(10), 1355 – 1364.

Muller, G., 1985, The reflectivity method: a tutorial: Journal of Geophysics, **58**, 153 – 174.

Ostrander, W. J., 1984, Plane wave reflection coefficients for gas sands at nonnormal angles of incidence: Geophysics, **49**, 1637 – l 648.

Rutherford, S. R., and Williams, R. H., 1989, Amplitude-versus-offset variations in gas sands: Geophysics, **54**(6), 680 – 688.

Shuey, R. T., 1985, A simplification of the Zoeppritz equations: Geophysics, **50**, 609 – 614.

Wei, X. C., Chen, T. S., and Ji, Y. X., 2008, Converted wave AVO inversion for average velocity ratio and shear wave reflection coefficient: 78th Annual International Meeting, SEG, Expanded Abstracts, 269 – 273.

Yang, P. J., Mu, X., and Yin, X. Y., 2009, Prestack three-term simultaneous inversion method and its application: Acta Petrolei Sinica, **30**(2), 232 – 236.

Yan, Z., and Gu, H. M., 2010, Application of quantum-behaved particle swarm optimization algorithm in AVO inversion: Oil Geophysical Prospecting, **45**(4), 516 – 519.

Zhang, F. C., and Yin, X. Y., 2004,A full wave field forward modeling and inversion method for prestack seismogram: Oil Geophysical Prospectin, **43**(3), 217 – 222.

Zhang, F. C., and Yin, X. Y., 2005, Elastic equation inversion of seismic data in layered half-space: Oil Geophysical Prospecting, **40**(5), 523 – 529.

Zoeppritz K. 1919, On the reflection and penetration of seismic waves through unstable layers. Goettinger Nachr, **I**, 66 – 84.

Appendix A

Derivation of geometric spreading factor

Bleistein et al. (2001) derived the geometric spreading factor for acoustic media. A geometric spreading factor derivation in a horizontal layered elastic medium is presented here. According to Snell's law, we have the ray parameter

$$p = \frac{\sin\theta(z)}{v(z)} = \frac{\sin\theta_{pi}}{v_{pi}} = \frac{\sin\theta_{si}}{v_{si}}. \qquad \text{(A-1)}$$

The PS wave offset is

$$x=\left(\int_0^z \frac{pv_p(z)}{\left[1-p^2v_p^2(z)\right]^{1/2}}dz+\int_0^z \frac{pv_s(z)}{\left[1-p^2v_s^2(z)\right]^{1/2}}dz\right), \tag{A-2}$$

where $v_p(z)$ and $v_s(z)$ are the P- and S-wave velocities.

For a horizontal layered medium, the ray horizontal distance in the i-th layer can be written as

$$\begin{aligned} x_i &= \int_{z_{i-1}}^{z_i} \tan\theta_p(z)\,dz+\int_{z_{i-1}}^{z_i} \tan\theta_s(z)\,dz \\ &= \int_{z_{i-1}}^{z_i} \frac{pv_p(z)}{\left[1-p^2v_p^2(z)\right]^{1/2}}dz+\int_{z_{i-1}}^{z_i} \frac{pv_s(z)}{\left[1-p^2v_s^2(z)\right]^{1/2}}dz, \end{aligned} \tag{A-3}$$

where $\tan\theta_p(z)$ and $\tan\theta_p(z)$ are the included angles between the P-wave ray, S-wave ray, and vertical direction, respectively.

Substituting equation (A-3) into equation (A-2), we get

$$x=\sum_{i=1}^{K} x_i=\sum_{i=1}^{K}\left(\int_{z_{i-1}}^{z_i} \frac{pv_p(z)}{\left[1-p^2v_p^2(z)\right]^{1/2}}dz+\int_{z_{i-1}}^{z_i} \frac{pv_s(z)}{\left[1-p^2v_s^2(z)\right]^{1/2}}dz\right). \tag{A-4}$$

Then, the equation (A-4) summation form can be written as

$$x=\sum_{i=1}^{K} x_i=\sum_{i=1}^{K}\left(\frac{pv_{pi}h_i}{\left(1-p^2v_{pi}^2\right)^{1/2}}+\frac{pv_{si}h_i}{\left(1-p^2v_{si}^2\right)^{1/2}}\right). \tag{A-5}$$

Where h_i is the thickness of the i-th layer, v_{pi} and v_{si} are the P-wave velocity and S-wave velocity of the i-th layer, respectively.

$$\frac{\partial p}{\partial\theta(M_0)}=\frac{\cos\theta(M_0)}{v_{p1}}, \tag{A-6}$$

Where $\theta(M_0)$ is the angle between the initial entering direction and vertical direction.

From equation (A-2), we get

$$\frac{\partial x}{\partial p}=\left(\int_0^z \frac{v_p(z)}{\left[1-p^2v_p^2(z)\right]^{3/2}}dz+\int_0^z \frac{v_s(z)}{\left[1-p^2v_s^2(z)\right]^{3/2}}dz\right) \tag{A-7}$$

and

$$\begin{aligned} \frac{\partial x}{\partial\theta(M_0)} &= \frac{\partial x}{\partial p}\frac{\partial p}{\partial\theta_{M_0}}=\frac{\cos\theta(M_0)}{v_{p1}} \\ &\times\left(\int_0^z \frac{v_p(z)}{\left[1-p^2v_p^2(z)\right]^{3/2}}dz+\int_0^z \frac{v_s(z)}{\left[1-p^2v_s^2(z)\right]^{3/2}}dz\right). \end{aligned} \tag{A-8}$$

Equation (A-8) can also be written as

$$\frac{\partial x}{\partial\theta(M_0)}=\frac{\cos\theta(M_0)}{v_{p1}}\sum_{i=1}^{K}\left(\frac{v_{pi}h_i}{\left(1-p^2v_{pi}^2\right)^{3/2}}+\frac{v_{si}h_i}{\left(1-p^2v_{si}^2\right)^{3/2}}\right). \tag{A-9}$$

Substituting equations (A-5) and (A-9) into equation (4), the PS wave geometric spreading factoris obtained.

$$\begin{aligned} L(M) &= \left[\sum_{i=1}^{K}\left(\frac{pv_{pi}h_i}{\left(1-p^2v_{pi}^2\right)^{1/2}}+\frac{pv_{si}h_i}{\left(1-p^2v_{si}^2\right)^{1/2}}\right)\right]^{1/2} \\ &\times\left[\frac{\cos\theta(M_0)}{v_{p1}}\sum_{i=1}^{K}\left(\frac{v_{pi}h_i}{\left(1-p^2v_{pi}^2\right)^{3/2}}+\frac{v_{si}h_i}{\left(1-p^2v_{si}^2\right)^{3/2}}\right)\right. \\ &\left.\times\frac{\cos\theta(M)}{\sin(M_0)}\right]^{1/2}\prod_{k=1}^{K}\left[\frac{\cos\theta(O_{k^+})}{\cos\theta(O_{k^-})}\right]^{1/2}. \end{aligned} \tag{A-10}$$

Then, we get

$$\begin{aligned} L(M) &= \left[\sum_{i=1}^{K}\left(\frac{v_{pi}h_i}{\left(1-p^2v_{pi}^2\right)^{1/2}}+\frac{v_{si}h_i}{\left(1-p^2v_{si}^2\right)^{1/2}}\right)\right]^{1/2} \\ &\times\left[\frac{\cos\theta(M_0)\cos\theta(M)}{v_{p1}^2}\sum_{i=1}^{K}\left(\frac{v_{pi}h_i}{\left(1-p^2v_{pi}^2\right)^{3/2}}\right.\right. \\ &\left.\left.+\frac{v_{si}h_i}{\left(1-p^2v_{si}^2\right)^{3/2}}\right)\right]^{1/2}\prod_{k=1}^{K}\left[\frac{\cos\theta(O_{k^+})}{\cos\theta(O_{k^-})}\right]^{1/2}. \end{aligned} \tag{A-11}$$

For PP-waves, in the case of horizontal layered media, ray paths are symmetric. The equation $\prod_{k=1}^{K}\left[\frac{\cos\theta(O_{k^+})}{\cos\theta(O_{k^-})}\right]^{1/2}$ is equivalent to 1. Changing v_{si} by

v_{pi} in equation (A-11), the PP-wave geometric spreading factor is obtained

$$L(M)=\left[\sum_{i=1}^{K}\left(\frac{2v_{pi}h_i}{\left(1-p^2v_{pi}^2\right)^{1/2}}\right)\right]^{1/2} \times\left[\frac{\cos\theta(M_0)\cos\theta(M)}{v_{p1}^2}\sum_{i=1}^{K}\left(\frac{2v_{pi}h_i}{\left(1-p^2v_{pi}^2\right)^{3/2}}\right)\right]^{1/2}. \quad \text{(A-12)}$$

Doing further simplification, we get

$$L(M)=\frac{2}{v_{p1}}\left[\sum_{i=1}^{K}\left(\frac{v_{pi}^2h_i^2}{\left(1-p^2v_{pi}^2\right)^2}\right)\cos\theta(M_0)\cos\theta(M)\right]^{1/2}. \quad \text{(A-13)}$$

Appendix B

Derivation of complex travel time in viscoelastic medium

The monochromatic plane wave in a viscoelastic medium is represented by

$$A(r)=A_0\exp(j\omega t)\exp((-\alpha-jk)r), \quad \text{(B-1)}$$

where α is the absorption coefficient, k is the wave-number, r is the propagation distance, $A(r)$ is the monochromatic wave amplitude after propagating distance r, and A_0 is the monochromatic plane wave initial amplitude.

Equation (B-1) can be written as

$$A(r)=A_0\exp(j\omega t)\exp\left(\left(-\frac{\alpha}{k}-j\right)kr\right). \quad \text{(B-2)}$$

Substituting $k=\frac{\omega}{v}=\frac{2\pi f}{v}$ into equation (B-2), we get

$$A(r)=A_0\exp(j\omega t)\exp\left(\left(-\frac{\alpha v}{2\pi f}-j\right)kr\right). \quad \text{(B-3)}$$

Substituting the relationship between quantity factor and absorption coefficient $Q=\frac{\pi f}{\alpha v}$ into equation (B-3), we get

$$A(r)=A_0\exp(j\omega t)\exp\left(\left(-\frac{1}{2Q}-j\right)kr\right). \quad \text{(B-4)}$$

We define complex travel time as

$$\tau_c=\tau\left(1-\frac{j}{2Q}\right), \quad \text{(B-5)}$$

where $\tau=\frac{r}{v}$.

Substituting equation (B-5) into (B-4), we get

$$A(r)=A_0\exp(j\omega(t-\tau_c)). \quad \text{(B-6)}$$

For horizontal layered media, the complex travel time of the k-th interface can be written as

$$\tau_c=\sum_{i=1}^{K}\tau_i\left(1-\frac{j}{2Q}\right), \quad \text{(B-7)}$$

where $\tau_i=\frac{h_i}{v_i}\left(1-p^2v_i^2\right)^{1/2}$.

Substituting equation (B-7) into equation (2) the wave equation zero-order asymptotic solution in a viscoelastic medium is obtained

$$\mathrm{u}(M,t)=\frac{1}{2\pi}\mathrm{Re}\int_0^{\infty}\left(S(\omega)e^{i\omega\left[t-\tau_c(M)\right]}W_0(M)\right)d\omega, \quad \text{(B-8)}$$

where $\tau_c(M)$ is calculated by equation (B-7) and other parameters are the same as those in elastic media.

Hou Bo is a doctorate student at China University of Petroleum (Beijing). His major is geophysical prospecting and his research work is mainly seismic wave propagation, imaging, and pre-stack seismic inversion.